# Lattice Boltzmann model for predicting the deposition of inertial particles in turbulent channel flows

Guillaume Lepoutère, Pascal Fede, Victor Sofonea, Richard A Fournier, Stéphane Blanco, Olivier Simonin

# Lattice Boltzmann model for predicting the deposition of inertial particles in turbulent channel flows

**Guillaume Lepoutère[1], Pascal Fede[1], Victor Sofonea[2], Richard Fournier[3], Stéphane Blanco[3], Olivier Simonin[1]**

[1]*Institut de Mécanique des Fluides de Toulouse (IMFT) - Université de Toulouse, CNRS, INPT, UPS, FR-31400 Toulouse, France*
[2]*Center for Fundamental and Advanced Technical Research, Romanian Academy, RO-300223 Timisoara, Romania*
[3]*Laboratoire Plasma et Conversion d'Energie (LAPLACE) - Université de Toulouse, CNRS, INPT, UPS, FR-31062 Toulouse, France*

Abstract

The purpose of the paper is the using of a Lattice Boltzmann Model (LBM) for solving the kinetic equation describing the interaction of solid inertial particles with a turbulent flows. The method has been successfully used for particles transported by a homogeneous isotropic turbulent flow field. In the present paper the LBM is used for the prediction of the particle deposition in vertical channel. In such a configuration, according to the Stokes number, the particle agitation may vary strongly with respect to the wall distance through the boundary layer that can be a problem for the LBM. However, the comparison of experimental data with the LBM results show that the deposition rate of particle is well predicted for large Stokes number (inertia dominated regime) and also for moderate Stokes number (impaction-diffusion regime).

*Keywords: LBM, gas-particle interaction, deposition, kinetic equation*

## 1. Introduction

Solid inertial particles suspended in turbulent flows are found in many practical applications as sediment transport or ripple motion, coal combustion, particulate radioactive contamination, pollutant deposition, drug inhalation by medicine aerosols.

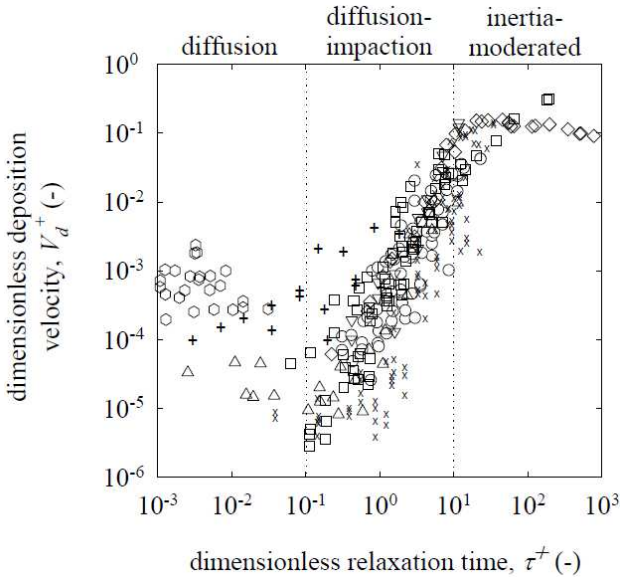


Figure 1: Particle deposition measured in several experiments and gathered by Sippola & Nazaroll [20] .

As shown by Figure 1, the particle deposition in turbulent channel flow can be split in three regimes [7]:

- $\tau_p^* << 1$: the diffusion regime where the particles behave like tracers and the deposition rate is controlled by the Brownian motion.
- $\tau_p^* >> 40$: the inertial regime, also called ballistic regime, where the particles do not interact with the turbulence, and achieve a free flight-like march down to the wall,
- $1 < \tau_p^* < 40$: the intermediate regime, also called diffusion-impaction regime, corresponding to a partial interaction of the particles with the turbulence.

where $\tau_p^* = \tau_p u^{*2}/\nu_f$ is the Stokes number with $\nu_f/u^{*2}$ the characteristic wall-turbulence time scale defined on the basis of a wall friction velocity $u^*$. Finally $\tau_p$ is the particle relaxation time

$$\tau_p = \frac{\rho_p d_p^2}{18\rho_f \nu_f} \ . \tag{1}$$

In parallel to experiments, Direct Numerical Simulation (DNS) or Large Eddy Simulation (LES) coupled with Discrete Particle Simulation (DPS) have been carried out for understanding the local mechanisms involved in particle deposition [12, 24, 11]. These numerical simulations have supported the development of modelling approaches for predicting the deposition rate of solid particles transported by a turbulent flow [21, 2, 25, 17].

In 2009, Aguinaga et al. [1] have proposed an original approach for modelling the dynamic behaviour of solid particles interacting with a turbulent flow. The approach, briefly described in the following section, is based on a statistical description of the particle motion by using a Probability Density Function (PDF). The originality of the approach lie in the closure of the gas-particle interaction term. Indeed that term is separated in two contributions: one for the mean gas-particle interaction and another one for the fluctuating gas-particle interaction. By making an analogy with the BGK model for rarefied gases, the fluctuating contribution is written as an return-to-equilibrium term. Under these closed form, the PDF transport equation can be solve and Aguinaga et al. [1] have shown that this can numerically unstable when the particle Stokes number becomes small. Diounou et al. [5] and later Fede et al. [6] have proposed to use a Lattice Boltzmann Model (LBM). They showed that LBM is able to predict the correct particle deposition in case where the turbulent flow is homogeneous and isotropic.

In the present study the same modelling approach and the same Lattice Boltzmann Model is used but in the case of a ver-

tical turbulent channel flow. In such a configuration, the turbulent properties (fluid agitation and dissipation) vary strongly from the top to the bottom of the turbulent boundary layer. Then the gas-particle interaction vary as well and the ability of the LBM approach may be questionable because the LBM have been developed for equilibrium flows. These issues are discussed in the present paper.

## 2. Modelling approach

The modelling approach is based on a statistical description of the particulate phase transported by a turbulent fluid flow. The dispersed phase is described by the particle Probability Density Function $f_p(\mathbf{x}, t; \mathbf{c}_p)$ defined such that $f_p(\mathbf{x}, t; \mathbf{c}_p) d\mathbf{c}_p d\mathbf{x}$ is the mean probable number of particles at the time $t$ with a centre of mass located in the volume $[\mathbf{x}, \mathbf{x} + d\mathbf{x}]$, with a translation velocity $\mathbf{u}_p$ in $[\mathbf{c}_p, \mathbf{c}_p + d\mathbf{c}_p]$. From the PDF the mean density number of particles writes

$$n_p = \int f_p d\mathbf{c}_p \, , \tag{2}$$

the mean particle velocity,

$$U_{p,i} = \frac{1}{n_p} \int c_{p,i} f_p d\mathbf{c}_p \, , \tag{3}$$

and the particle kinetic stress,

$$\langle u'_{p,i} u'_{p,j} \rangle = \frac{1}{n_p} \int [c_{p,i} - U_{p,i}] \times [c_{p,j} - U_{p,j}] f_p d\mathbf{c}_p \, . \tag{4}$$

The single particle velocity PDF obeys to the following Boltzmann-like kinetic equation:

$$\frac{\partial f_p}{\partial t} + \frac{\partial}{\partial x_i} \left[ c_{p,i} f_p \right] + \frac{\partial}{\partial c_{p,i}} \left[ \left\langle \frac{du_{p,i}}{dt} | \mathbf{c}_p \right\rangle f_p \right] = \left( \frac{\partial f_p}{\partial t} \right)_{col} \tag{5}$$

where $\langle . | \mathbf{c}_p \rangle$ is the ensemble average conditioned by the particle velocity and $i$ is a summation index. In Eq. (5), the third term on the left-hand-side represents the forces acting on the particles, including the turbulent particle-fluid coupling, and the term on the right-hand-side is the modification of the PDF by the inter-particle collisions. In the present study the particulate phase is very dilute such that this term can be safely neglected. Assuming a large particle-to-fluid density ratio, the forces acting on the particles are reduced to the gravity and the drag. In such a framework, the particle acceleration reads

$$\frac{d\mathbf{u}_p}{dt} = -\frac{\mathbf{u}_p - \mathbf{u}_{f@p}}{\tau_p} + \mathbf{g} \tag{6}$$

where $\mathbf{u}_{f@p}$ is the fluid velocity at the particle position, $\mathbf{g}$ the gravity and $\tau_p$ the particle relaxation time.

In the following the PDF transport equation is simplified to the case of a particle-turbulence interaction in a wall boundary layer flow then it can be assumed that $\partial/\partial y \approx \partial/\partial z \approx 0$. Also as $\tau_p$ has a given value independent of the instantaneous particle velocity, the kinetic equation governing the wall-normal particle velocity PDF is obtained by integration of Eq. (5) on the velocity components in $y-$ and $z-$directions. Using Eq. (6) in the third term of Eq. (5) and neglecting gravity, the Boltzmann equation becomes

$$\frac{\partial f_p}{\partial t} + \frac{\partial}{\partial x} \left[ c_p f_p \right] + \frac{\partial}{\partial c_p} \left[ -\frac{1}{\tau_p} (c_p - \langle u_{f@p} | c_p \rangle) f_p \right] = 0 \tag{7}$$

where $c_p$ is the particle velocity component expectation in the $x$-direction normal to the wall.

The literature dedicated to the modelling of the particle-turbulence coupling in the kinetic equation is abundant [4, 26, 15, 16, 18]. As explained in introduction, the closure is done by the approach proposed by Aguinaga et al. (2009) [1] where the fluid-particle interaction term is split in two contributions: first, the fluid-particle interaction through the mean gas and particle velocities; second, the coupling of the particle fluctuating motion with the fluid turbulence. The last contribution is modelled as a return-to-equilibrium term in a similar manner to the effect the inter-particle interactions in the BGK model [3]. The return-to-equilibrium term requires an equilibrium PDF, $f^*$, and a given time-scale, $\tau^*$. As shown by Aguinaga et al. (2009) [1], for being consistent with the standard moment equation the time-scale, $\tau^*$, is the particle response time $\tau_p$. The fluid-particle interaction is then written as

$$\begin{aligned} \frac{\partial}{\partial c_p} \left[ -\frac{1}{\tau_p} (c_p - \langle u_{f@p} | c_p \rangle) f_p \right] = & - \left[ \frac{U_p - U_{f@p}}{\tau_p} \right] \frac{\partial f_p}{\partial c_p} \\ & + 2 \frac{f_p - f^*}{\tau_p} \, . \end{aligned} \tag{8}$$

The equilibrium PDF, $f^*$, is chosen in order to model particles in equilibrium with the gas turbulence according to the Tchen & Hinze theory [22, 8]:

$$\langle u'_p u'_p \rangle = \langle u'_{f@p} u'_p \rangle = \langle u'_{f@p} u'_{f@p} \rangle \frac{1}{1 + St} \tag{9}$$

with the Stokes number $St = \tau_p / \tau^t_{f@p}$ where $\tau^t_{f@p}$ is the fluid Lagrangian integral time scale seen by the particles. As shown later, the modelling of the such a timescale in turbulent boundary layer is crucial for the particle dispersion. The equilibrium PDF is modelled by a Gaussian distribution [9]

$$f^*(x, t; c_p) = \frac{n_p}{\left( 2\pi \left\langle u'_{f@p} u'_p \right\rangle \right)^{1/2}} \exp \left[ -\frac{(c_p - U_p)^2}{2 \left\langle u'_{f@p} u'_p \right\rangle} \right] \, . \tag{10}$$

The mean fluid velocity seen by the particles, $U_{f@p}$, has two contributions: i) the mean fluid velocity $U_f$ and ii) a drift velocity $U_{drift}$ representing the correlation between the local instantaneous particle distribution and the turbulent fluid velocity. Then the mean fluid velocity seen by the particles is written as $U_{f@p} = U_f + U_{drift}$ and, following Simonin et al. [19], the drift velocity in homogeneous turbulence reads,

$$U_{drift} = -\tau^t_{f@p} \left\langle u'_{f@p} u'_p \right\rangle \frac{1}{n_p} \frac{\partial n_p}{\partial x} \, . \tag{11}$$

Finally the Boltzmann-like transport equation (7) with the SAB model for the fluid-particle interaction writes

$$\frac{\partial f_p}{\partial t} + c_p \frac{\partial f_p}{\partial x} - \left[ \frac{U_p - (U_f + U_{drift})}{\tau_p} \right] \frac{\partial f_p}{\partial c_p} + \frac{2}{\tau_p} \left[ f_p - f^* \right] = 0 \, . \tag{12}$$

## 3. Lattice Boltzmann Model (LBM)

The Lattice Boltzmann model used to solve the Eq. (12) is described by Fede et al. [6]. Basically, an approximate form of Eq. (12) is used in which the distribution function $f_p$ appearing in the force term is replaced by a Hermite polynomial expansion of kernel $f^0_p$, where

$$f^0_p = \frac{n_p}{\sqrt{2\pi \left\langle u'_p u'_p \right\rangle}} \exp \left[ -\frac{(c_p - U_p)^2}{2 \left\langle u'_p u'_p \right\rangle} \right] \tag{13}$$

is the local equilibrium distribution function. Then Boltzmann equation projected onto Hermite polynomial basis reads

$$\frac{\partial f_p}{\partial t} + c_p \frac{\partial f_p}{\partial x} - \left[\frac{U_p - (U_f + U_{drift})}{\tau_p}\right] \frac{\partial}{\partial c_p}\left(Q_{N_h} f_p^0\right) + \frac{2}{\tau_p}\left[f_p - f^*\right] = 0 \quad (14)$$

where $Q_{N_h}$ is a polynomial function of $c_p$ of order $N_h$ (the Hermite expansion order) that depends on all moments of the distribution function of order lower or equal to $N_h$ and $f^*$ is now the its projection onto the Hermite polynomial basis. Then procedure allows to replace the partial derivative $\partial f_p/\partial c_p$ by an explicit function of the moments,transforming the question of choosing a set of discrete velocities into a quadrature choice.

The second step is the quadrature choice itself. Equation 14 involves the following integral quantities appearing in $f_p^0$ and $f^*$, and all the moments of the vector appearing in $Q_{N_h}$. This means that the question is only the evaluation of velocity moments of increasing orders. Here, a Gauss-Hermite quadrature of order $N_q$ is used. Altogether, $N_q$ values $f_{p,\alpha}$ of the distribution function ($\alpha = 1, 2, ...N_q$), at discrete velocities $\check{c}_{p,\alpha}$, are considered in their coupled temporal evolutions according to

$$\frac{\partial f_{p,\alpha}}{\partial t} + \check{c}_{p,\alpha}\frac{\partial f_{p,\alpha}}{\partial x} - \left[\frac{U_p - (U_f + U_{drift})}{\tau_p}\right]\left[\frac{\partial}{\partial c_p}\left(Q_{N_h} f_p^0\right)\right]_{c_p = \check{c}_{p,\alpha}} + \frac{2}{\tau_p}\left[f_{p,\alpha} - f_\alpha^*\right] = 0 \quad (15)$$

where $U_p$, $Q_{N_h}$ and $f_\alpha^*$ are the approximations of the corresponding terms in Eq. (14) in which all the moments $M_m$ are replaced by their evaluation as $\sum_{\alpha=1}^{N_q} \omega_\alpha f_{p,\alpha} \check{c}_{p,\alpha}^m$ where $\omega_1$, $\omega_2$, ..., $\omega_{N_q}$ are the $N_q$ quadrature weights. $\alpha$ is a free index.

## 4. Numerical simulation overview

The configuration is an established vertical turbulent channel flow obtained thanks to the DNS of Moser et al. [13]. The deposition rate will be compared to the one obtained by Liu & Agarwal [10].

### *4.1. Geometry, mesh and boundary conditions*

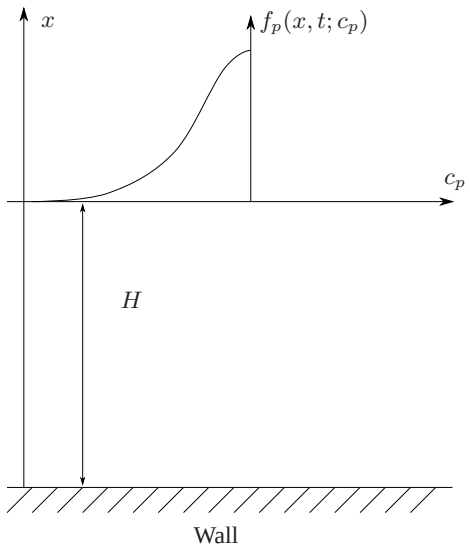


Figure 2: Computational domain.

As explained previously, the problem is one-dimensional in space and one-dimensional in velocity (wall-normal component). The size of the computational domain, shown by Figure 2, is denoted $H$ (the half-width of the channel is located at $x = H$ and the wall at $x = 0$). As the flow is heterogeneous, a non uniform mesh having 200 cells is used. The mesh is refined close to the wall.

At the top of the domain, the PDF entering in the domain, namely for $c_p < 0$, is imposed as

$$f(x = H, t; c_p < 0) = \frac{n_p}{\left(2\pi \left\langle u'_{f@p} u'_p \right\rangle\right)^{1/2}} \times \exp\left[-\frac{c_p^2}{2\left\langle u'_{f@p} u'_p \right\rangle}\right] . \quad (16)$$

At the wall, a full absorption wall condition is imposed meaning that no particle are going back to the flow. This condition reads

$$f(x = 0, t; c_p > 0) = 0 . \quad (17)$$

### *4.2. Fluid flow*

In the present study, the fluid flow is imposed through its moments (in terms of mean velocity, mean Reynolds stress, and dissipation). Then in order to avoid of using a model for the prediction of the turbulent flow the profiles that Moser et al. [13] obtained by DNS have been used.

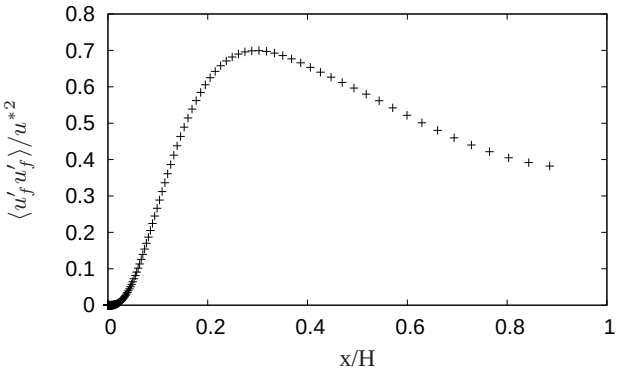


Figure 3: Wall-normal fluid agitation measured by Moser et al. [13] in DNS.

Figure 3 shows the wall-normal Reynolds stress component with respect to the wall distance. As expected in the near wall region $\langle u'_f u'_f \rangle$ decreases quickly up to reach zero at the wall. The Reynolds number

$$Re_\tau = \frac{H\, u^*}{\nu_f} \quad (18)$$

based on frictional velocity, $u^*$, and the half-width of the channel is 180 and the dimensionless particle diameters $d_p* = d_p u*/\nu_f$ vary between $3.10^{-2}$ and $2.9$. The Reynolds numbers of the Liu & Agarwal [10] experiment is 309 and 1308 and the dimensionless particle diameters $d_p*$ vary between $7.10^{-2}$ and 1 for the first Reynolds number and between $0.28$ and $4.2$ for the second.

The modelling approach has two input parameters: the gas-particle velocity covariance $\langle u'_{f@p} u'_p \rangle$ and the integral timescale of the fluid turbulence seen by the particles $\tau^t_{f@p}$. The gas-particle covariance is computed by assuming the local equilibrium (Tchen-Hinze theory)[23]. Following this, the gas-particle

covariance is given in terms of the wall-normal Reynolds stress as

$$\langle u'_{f@p} u'_p \rangle = \langle u'_{f@p} u'_{f@p} \rangle \frac{\tau^t_{f@p}}{\tau^t_{f@p} + \tau_p} \tag{19}$$

with $\langle u'_{f@p} u'_{f@p} \rangle \approx \langle u'_f u'_f \rangle$. In a first approximation the fluid integral timescale seen by the particles is assumed to be equal to the one of the fluid $\tau^t_{f@p} \approx \tau^t_f$.

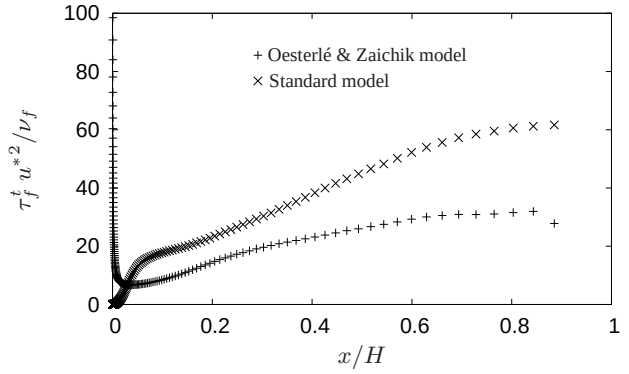


Figure 4: Lagrangian fluid integral time scale predicted by the standard model (+) and by the Oesterlé & Zaichik Model (×) [14].

In the framework of the RANS approach, the Lagrangian fluid integral time scale is commonly computed from the fluid agitation and dissipation as

$$\tau^t_f = \frac{1}{2}\frac{k}{\varepsilon}\,. \tag{20}$$

Oesterlé & Zaichik [14] proposed to estimate the Lagrangian fluid integral timescale by

$$\tau^t_f = -\frac{\langle u'_f v'_f \rangle}{\langle u'_f u'_f \rangle \frac{\partial V_f}{\partial x}} \tag{21}$$

where the gradient $\partial V_f/\partial x$ is given by the DNS data and the shear stress $\langle u'_f v'_f \rangle$ as well. Figure 4 shows the Lagrangian timescale given by Eq. (20) & (21) with respect to the wall-normal distance. In the near-wall region the standard model predicts that Lagrangian integral timescale tends to zero whereas the "eddy-viscosity" model proposed by Oesterlé & Zaichik [14] predicts that the timescale goes to infinity.

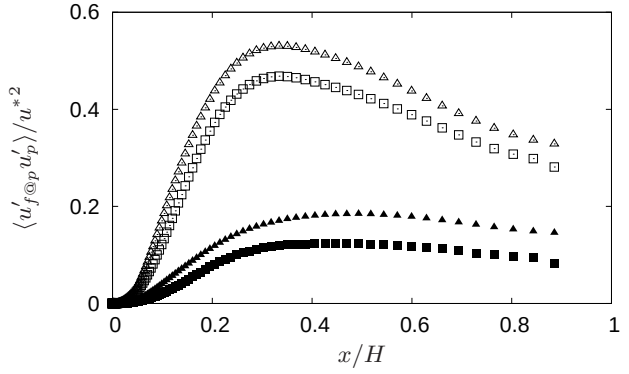


Figure 5: Wall-normal fluid-particle covariance predicted when using the standard model (triangles) and the Oesterlé & Zaichik [14] model (squares). Empty symbols: $\tau^*_p = 10$ and black-filled symbols $\tau^*_p = 100$.

The gas-particle covariance evolution with respect to the wall-normal distance is shown by Figure 5 for two Stokes number $\tau^*_p = 10$ and $\tau^*_p = 100$. As expected the larger the Stokes number is, the smaller the gas-particle covariance is. Figure 5 also shows that the model given by Eq. (21) leads to covariance slightly smaller than the predictions with Eq. (20).

### *4.3. Physical properties*

The Reynolds number is equal to 180. The Stokes number $\tau^*_p$ vary between $0.1$ and $1000$ and the dimensionless particle diameters vary between $2.9\ 10^{-2}$ and $2.9$.

### *4.4. LBM parameters*

The numerical simulation have been performed with 20 discrete velocities with $6th$ order polynomial Hermite expansion ensuring that the five first moments of $f_p$ are accurately computed [6].

## 5. Particle deposition in vertical channel flow

The deposition rate of particles transported in turbulent vertical channel flow is shown by Figure 6. In LBM simulations, we steady state is reached, the deposition rate is computed by

$$V^+_d = \frac{1}{u^*} \frac{\int^0_{-\infty} c_p f_p(x=0) dc_p}{\frac{1}{H}\int^H_0 \left[\int^{+\infty}_{-\infty} f_p dc_p\right] dy}. \tag{22}$$

Figure 6 shows that the LBM model predict the inertia-moderated regime, the diffusion-impaction regime and the transition between these two regimes. In diffusion-impaction regime the slope predicted by the LBM is in accordance with slope measured by Liu & Agarwal [10] in their experiments. However, the magnitude of the deposition rate is slightly overestimated by the LBM.

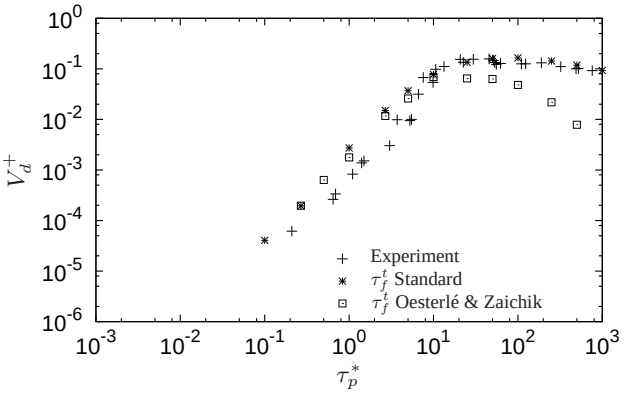


Figure 6: Deposition rate with respect to the Stokes number. Comparison between the experiments of Liu & Agarwal [10], the LBM prediction with $\tau^t_f$ predicted by the standard model (20) and by the model proposed by Oesterlé & Zaichik (21) [14].

It is also observed that in the impaction-diffusion regime the standard model for the Lagrangian fluid integral timescale gives the same predictions than the model of Oesterlé & Zaichik [14]. In contrast, some differences are shown by Figure 6 in inertia-moderated regime. Indeed, the "eddy-viscosity" model leads to an underestimation of the deposition whereas the standard model gives predictions in very good accordance with the experiments.

The mean density number of particles with respect to the wall-distance is shown by Figure 7. For small Stokes number ($\tau^*_p = 1$), the profile of $n_p$ is nearly flat from the centre of the

channel to $x/H = 0.2$. When approaching the wall the mean particle density number is increasing and reaches a maximum for $y^+ = 2.5$. Finally from $y^+ = 2.5$ up to $d_p/2$ the particle density is decreasing. For $\tau_p^* = 10$ the trends are the same excepted that in the core of the channel the particle number density is decreasing from the centre to the reach also a peak at $y^+ = 8$. Between $y^+ = 8$ and the wall, $n_p$ is decreasing an reaches a plateau. Finally for $\tau_p^* = 100$, the peak close to the wall vanishes.

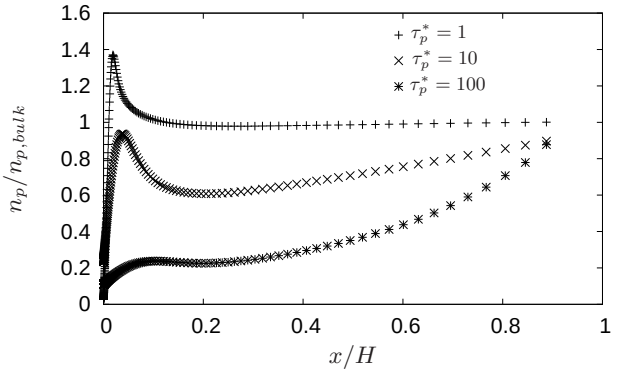


Figure 7: Mean particle number density predicted by LBM for $\tau_p^* = 1,\ 10,\ 100$ with respect to the normalized wall-distance.

Figure 8 shows the mean particle velocity with respect to the normalized wall-distance. As expected, when increasing $\tau_p^*$ the wall-normal mean particle velocity is increasing.

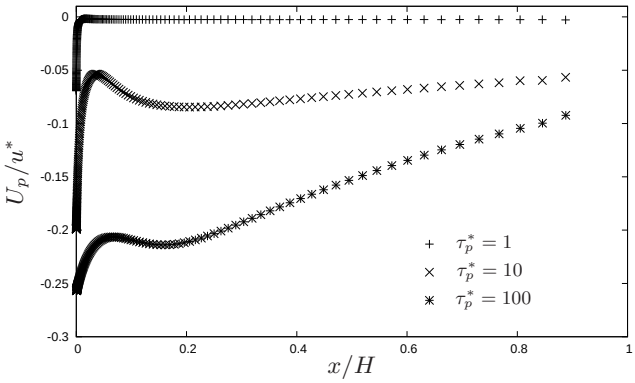


Figure 8: Mean particle velocity predicted by LBM for $\tau_p^* = 1,\ 10,\ 100$ with respect to the normalized wall-distance.

The particle velocity covariance is depicted by Figure 9. From the center of the channel towards the wall, the particle kinetic stress is increasing for reaching a peak that is closer to wall for smaller Stokes number. For $\tau_p^* = 100$ and $\tau_p^* = 10$ the variance reaches in a constant positive value very close to the wall. In contrast, for $\tau_p^* = 1$ the particle variance follows the same trend excepted that for $y^+ < 1$ the particle variance becomes negative that is not correct. It is possible that for such a small Stokes number the order of the quadrature has to be increased.

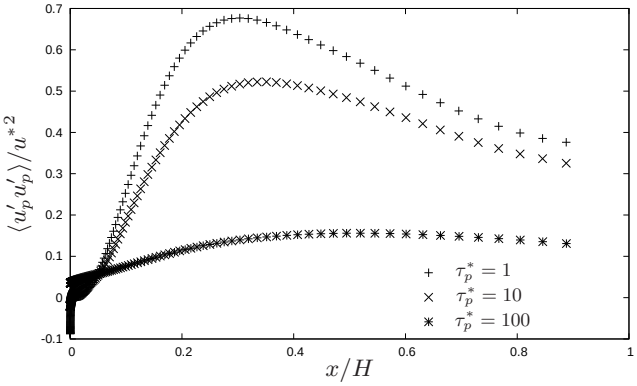


Figure 9: Mean particle variance density predicted by LBM for $\tau_p^* = 1,\ 10,\ 100$ with respect to the normalized wall-distance.

## 6. Conclusion

Lattice Boltzmann Model has been used for solving a kinetic equation describing the interaction of inertial particles with a turbulent flow. The LBM has been applied for predicting the deposition of particles interacting with a turbulent boundary layer. The results show that the deposition rate is in accordance with experimental data for the inertial and impaction-diffusion regime. The transition between inertial and impaction-diffusion regime is well predicted and the slope of the deposition rate is correct.These promising results show that the method seems to be able to predict correctly the gas-particle interaction in the near-wall region but more development are needed. Some trouble stay for the prediction of the moments in the near wall region and some complementary investigations are in progress. The influence of the Reynolds number on the deposition rate predicted by the method is also investigated. Future developments will include different wall interaction such as elastic bounce-back or the addition of the Brownian motion.

## 7. Acknowledgements

This work was supported by the ANR DEPART project, Grant ANR-12-IS04-0003-01 of the French Agence Nationale de la Recherche and the grant of the Romanian National Authority for Scientific Research CNCS-UEFISCDI, Project Number PN-II-ID-JRP-2011-2-0060.

## References

[1] S. Aguinaga, O. Simonin, J. Borée, and V. Herbert. A simplified particle-turbulence interaction pdf model: application to deposition modelling in turbulent boundary layer. In *Proceedings of the ASME 2009 Fluids Engineering Division Summer Meeting, August 2-6, 2009, Vail, Colorado USA*, pages 2–6, 2009.

[2] A. S. Berrouk and D. Laurence. Stochastic modelling of aerosol deposition for les of 90 bend turbulent flow. *International Journal of Heat and Fluid Flow*, 29:1010 – 1028, 2008.

[3] P. L. Bhatnagar, E. P. Gross, and M. Krook. A model for collision process in gases. i.small amplitude processes in charged and neutral one-component systems. *Physical Review*, pages 94–511, 1954.

[4] I. V. Derevich and L. I. Zaichik. Precipitation of particles from a turbulent flow. *Izvetiyia Akademii Nauk SSSR*

*Mekhanika Zhidkosti i Gaza*, 5:96–104, 1988.

[5] E. Diounou, P. Fede, R. Fournier, S. Blanco, and O. Simonin. Kinetic approach for solid inertial particle deposition in turbulent near-wall region flow lattice Boltzmann based numerical resolution. In *Proceedings of AJK2011-FED, ASME-JSME-KSME Joint Fluids Engineering Conference 2011, July 24-29, 2011, Hamamatsu, Shizuoka, JAPAN*, number AJK2011-12021, pages 3229–3238, 2011.

[6] P. Fede, V. Sofonea, R. Fournier, S. Blanco, O. Simonin, G. Lepoutère, and V. Ambrus. Lattice boltzmann model for predicting the deposition of inertial particles transported by a turbulent flow. *International Journal of Multiphase Flow*, 76:187 – 197, 2015.

[7] S. Friedlander and H. Johnstone. Deposition of suspended particles from turbulent gas stream. *Journal of Industrial and Engineering Chemistry*, 49:1159, 1957.

[8] J. O. Hinze. Turbulent fluid and particle interaction. *Prog. Heat and Mass Transfer*, 6:433–452, 1972.

[9] J. Laviéville, E. Deutsch, and O. Simonin. Large Eddy Simulation of interaction between colliding particles and a homogeneous isotropic turbulence field. In *6th Int. Symp. On Gas-Solid Flows*, volume 228, pages 347–357. ASME FED, 1995.

[10] B. Y. H. Liu and J. K. Agarwal. Experimental observation of aerosol deposition in turbulent flow. *Journal of Aerosol Science*, 5(2):145 – 155, 1974.

[11] C. Marchioli, M. Picciotto, and A. Soldati. Influence of gravity and lift on particle velocity statistics and transfer rates in turbulent vertical channel flow. *International Journal of Multiphase Flow*, 33:227 – 251, 2007.

[12] J. B. McLaughlin. Aerosol particle deposition in numerically simulated channel flow. *Physics of Fluids*, 7:1211–1224, 1989.

[13] R. D. Moser, J. Kim, and N. N. Mansour. Direct numerical simulation of turbulent channel flow up to ret=590. *Physics of Fluids*, 11(4):943–945, 1999.

[14] B. Oesterlé and L. I. Zaichik. On lagrangian time scales and particle dispersion modeling in equilibrium turbulent shear flows. *Physics of Fluids*, 16(9):3374–3384, 2004.

[15] M. W. Reeks. On the continuum equations for dispersed particles in nonuniform flows. *Physics of Fluids*, 4(6):1290–1303, 1992.

[16] M. W. Reeks. On the constitutive relations for dispersed particles in nonuniform flows. I : Dispersion in a simple shear flow. *Physics of Fluids*, 5:750–761, 1993.

[17] D. Sikovsky. Stochastic lagrangian simulation of particle deposition in turbulent channel flows. *Flow, Turbulence and Combustion*, 95(2-3):561–582, 2015.

[18] O. Simonin. Statistical and continuum modelling of turbulent reactive particulate flows. part 1 : Theoretical derivation of dispersed eulerian modelling from probability density function kinetic equation. In *Lecture Series 2000-06, Von Karman Institute for Fluid Dynamics, Rhodes Saint Genèse (Belgium)*, pages –. Von Karman Institute for Fluid Dynamics, 2000.

[19] O. Simonin, E. Deutsch, and J. P. Minier. Eulerian prediction of the fluid/particle correlated motion in turbulent two-phase flows. *App. Sci. Res.*, 51:275–283, 1993.

[20] M. R. Sippola and W. W. Nazaroff. Particle deposition from turbulent flow: Review of published research and its applicability to ventilation ducts in commercial buildings, 2002.

[21] D. C. Swailes and M. W. Reeks. Particle deposition from turbulent flow. i. a steady-state model for high inertia particles. *Physics of Fluids*, 6:3392–3403, 1994.

[22] C. M. Tchen. *Mean value and correlation problems connected with the motion of small particles suspended in a turbulent fluid*. PhD thesis, Delft, Martinus Nijhoff, The Hague, 1947.

[23] M. W. Vance, K. D. Squires, and O. Simonin. Properties of the particle velocity field in gas-solid turbulent channel flow. *Physics of Fluids*, 18:13, 2006.

[24] Q. Wang and K. D. Squires. Large eddy simulation of particle deposition in a vertical turbulent channel flow. *International Journal of Multiphase Flow*, 22:667–683, 1997.

[25] L. I. Zaichik, V. M. Alipchenkov, and A. R. Avetissian. Transport and deposition of colliding particles in turbulent channel flows. *International Journal of Heat and Fluid Flow*, 30:443–451, 2009.

[26] L. I. Zaichik, V. A. Pershukov, M. V. Kozelev, and A. A. Vinberg. Modeling of dynamics, heat transfer, and combustion in two-phase turbulent flows: 1. isothermal flows. *Experimental Thermal and Fluid Science*, 15(4):291 – 310, 1997.